Evaluation of a broadband marine source

Rob Telling, Stuart Denny, Sergio Grion and R. Gareth Williams, Dolphin Geophysical

Summary

Broadband air-gun arrays are designed to attenuate the source ghost and are expected to deliver improved bandwidth over conventional arrays. In this work, we evaluate far-field signatures and compare processing results for a 2D test-line acquired with an experimental broadband source and a standard source. The datasets were processed using essentially identical pre-stack time migration sequences and were quantitatively evaluated in terms of signal coherency. The results of our analysis show that the two datasets are of comparable quality. In both cases imaging in the shallow data is improved by extending conventional source bandwidth out to 200 Hz. The datasets acquired using standard and broadband sources differed most in their raw state and these differences were significantly reduced after processing. This indicates that both processing and array-based solutions can compensate well for the effect of the source ghost. However, the broadband source dataset is characterized by a modest improvement in signal quality that is apparent for frequencies in the vicinity of the standard source's ghost notch.

Introduction

A standard seismic source is comprised of an array of air-guns all placed at the same depth, so that all guns contribute to a single ghost response. The interference between primary and ghost can reduce bandwidth. Broadband air-gun arrays are designed to attenuate the source ghost by placing guns at a range of depths within the array which diversifies the frequencies at which the source ghost notch appears for each gun. This leads to a flatter spectrum and an expectation of improved bandwidth with respect to a standard source. We evaluate far-field signatures and compare processing results for a 2D test-line acquired with an experimental broadband source and a standard source. Parkes and Hegna, (2011) and Siliqi et al. (2012) have also recently studied the broadband array concept. Our investigation differs in the details of the processing and of the analysis of results. The standard source data we use as reference were processed up to the Nyquist frequency and not just up to the first source ghost notch frequency. This allows an objective assessment of the processing and broadband array solutions to the source ghost problem. The datasets were processed using essentially identical pre-stack time migration sequences, which included source- and receiver-side de-ghosting, and the data were then evaluated in terms of signal coherency.

Acquisition

2D seismic data were acquired for each source along the same 30 km sail line in the Norwegian part of the North Sea. The vessel was rigged with both sources firing alternately, thus minimizing any differences in the data due to weather, water velocity and cable feathering. The data acquired for each source were later separated for processing. The standard and broadband sources each comprised three strings with 6 cluster positions and 28 guns in total, ranging from 40 to 300 cubic inches. Total gun volume in each case was 4100 cubic inches. The air-guns in the standard array were all set at 7 m with identical timing. In the broadband source array the guns were deployed in a slanted configuration with depths ranging between 4.5 and 15.5 m. By appropriate timing of the guns, in the range 0.0 to 7.3 ms based on gun depth within the array, the downward leading wave-front was synchronized. Data were recorded at 2 ms sample interval via a 340 channel, 12.5 m spaced, hydrophone-only flat streamer at 30 m depth. The significant wave height recorded in the Observer's log was 3 m.

Source

Figure 1 shows the modelled in-line directivity as a function of frequency for each array with ghosts applied. For the standard source at vertical incidence, the first non-zero notch frequency appears at 107 Hz, corresponding to the condition for destructive interference between primary and ghost, with a path difference of twice the depth of the source array. The corresponding plot for the broadband source shows no such prominent notch, but also no constructive interference at frequencies away from the ghost notch i.e. a broadband source attenuates both the destructive and the constructive interference. In terms of signal penetration the broadband source provides a gain over the standard source in correspondence to the standard source's ghost notch frequencies, jointly with a loss at other frequencies. The right-hand plot in *Figure 1* illustrates this concept, showing the relative gain expected of the broadband source, as a function of frequency. The blue curve is for vertical incidence which shows considerable gain at the standard source ghost notch frequency and a corresponding loss for lower and higher frequencies. In practice however, a seismic image is formed by stacking reflections from a variety of angles, and both the source array response and the source ghost change with angle. To illustrate this point the red curve shows the theoretical gain as a function of frequency for a 50^{o} stack.

Data processing

To ensure objective comparison, the datasets were processed using an essentially identical pre-stack time migration sequence:

- 1.5 Hz/18 dB roll-off low-cut filter applied

- Noise and aliased energy attenuation using f-x and f-k filtering
- De-convolution of bubble pulse and zero-phasing of wavelet
- Multiple attenuation
- Source and receiver-side de-ghosting
- f-x de-convolution
- Kirchhoff pre-stack time migration
- Residual multiple and noise attenuation
- Stack
- Amplitude, time and phase - matching of the different datasets

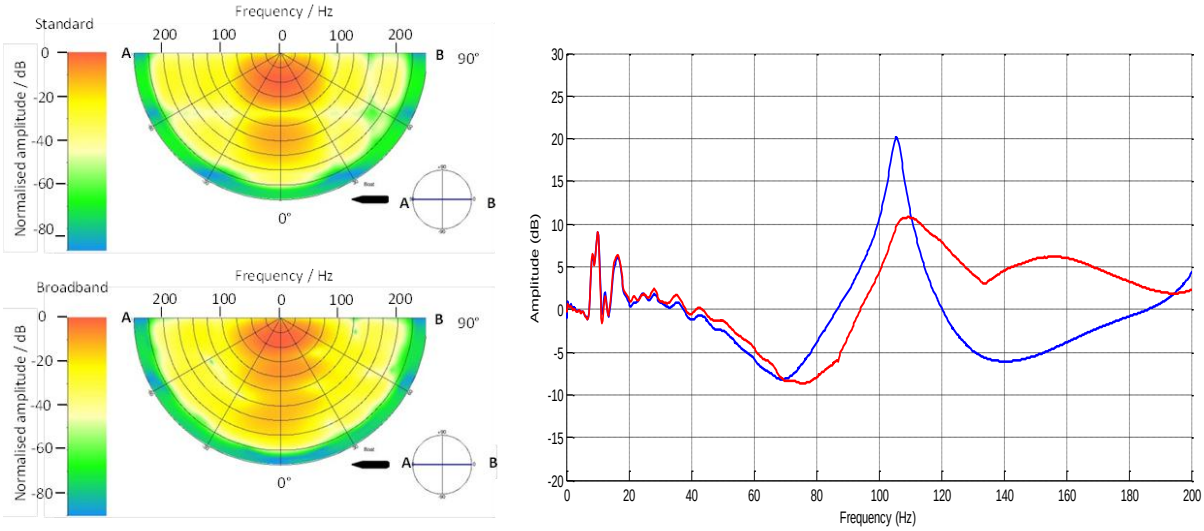

Figure 1 *– Left - Array directivity as a function of in-line take-off angle and frequency for the standard (top image) and broadband source (bottom image). Right – Theoretical relative gain of the broadband source over the standard source, at vertical incidence (blue) and for a 0^o to 50^o stack (red) as a function of frequency. The sea-surface reflection coefficient is R=-0.9.*

Results and analysis

Firstly, a comparison was made of the effect of processing the standard source data over the full available bandwidth 2-200 Hz versus processing only up to the first source notch i.e. 2-107 Hz bandwidth. Figure 2 shows a shallow section of the data. The arrows in the figure highlight some of the horizons that are resolved with full bandwidth available but which are not visible or poorly resolved for the band-limited case, showing that there is an advantage to using this greater bandwidth.

The fully-processed sections obtained with the broadband source and using the standard source are shown in Figure 3 and appear broadly comparable from a structural imaging point of view. The similarity is due to the processing effort in attenuating ghost arrivals in both datasets, as well as to the noise and multiple attenuation sequences. Frequency-dependent differences are not easily identifiable in the images. To investigate the relative merits of the two datasets further, and taking into account the relative gain curves in Figure 1, we focus on the frequency range where the greatest difference between the datasets is expected. We apply a narrow 102-112 Hz band-pass filter to the data, with a roll-off of 72 dB/octave. These filtered datasets are shown in Figure 4, and it is apparent that some improvement is obtained with the broadband source, where a greater lateral coherence and signal strength is evident for events in the shallow data.

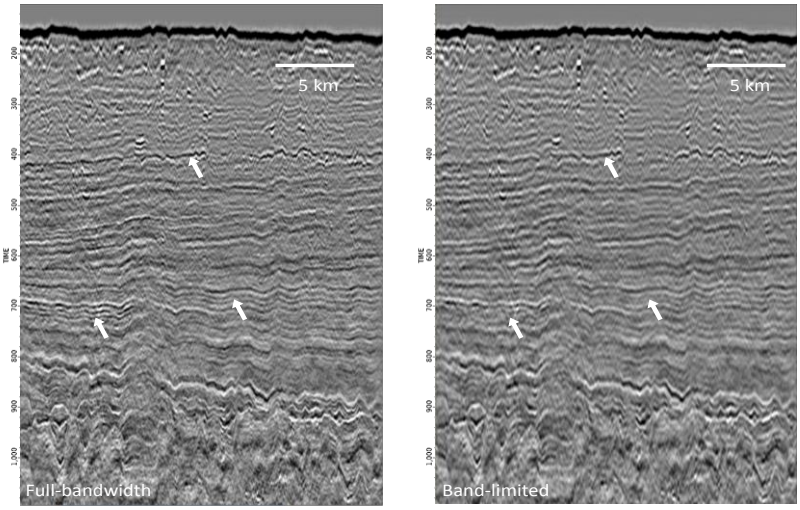

Figure 2 *– Shallow (0-1000 ms) PSTM stack of standard source data processed to full bandwidth (left) and band-limited to the standard source ghost notch (right). Arrows indicate areas where differences in resolution are particularly evident.*

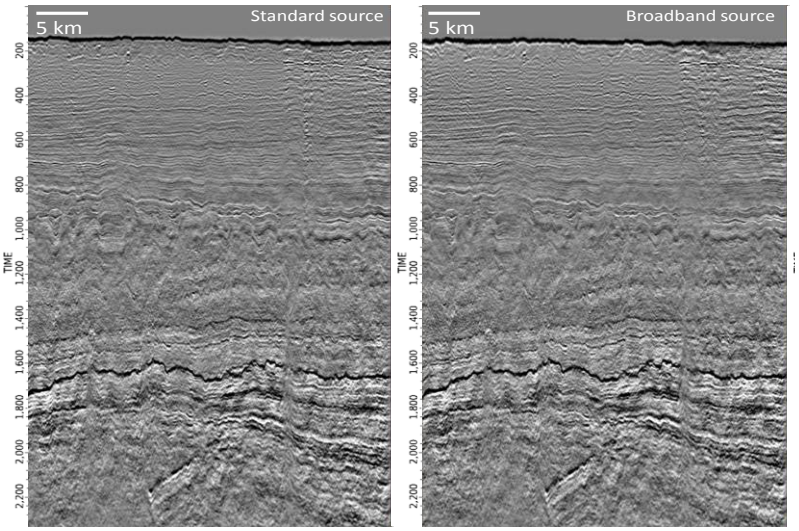

Figure 3 *– PSTM stack of standard source data (left) and broadband source data (right) showing broadly very similar structural imaging.*

To quantify this small improvement in the 102-112 Hz band and extend the analysis of the two datasets over the whole frequency range, a signal-to-noise (SNR) ratio estimate was derived. The SNR estimate is based on the predictability attribute (see for example Kragh and Christie, 2002). This was also carried out on the raw data before processing. These results are shown in Figure 5. The relative SNR gain curve for the raw data shows alternating peaks and troughs that resemble those shown in Figure 1 (right), and can be attributed to the different performance of the two sources in different frequency bands. On the other hand, the SNR for the processed data shows smaller differences between datasets. Nevertheless, a modest advantage is seen for the broadband source data over the standard data of the order of 0.5 to 1 dB in the band 50-150 Hz, consistent with the qualitative comparison and broader, although less pronounced, than the theoretical gains predicted earlier. In terms of low frequencies, the 2-2.5dB gain of the broadband source over the standard in the raw data appears to have been equalized by our processing sequence.

Conclusions

Imaging in the shallow data is improved by extending conventional source bandwidth, which is evident for this survey for two-way times up to 1000 ms. The datasets acquired using standard and broadband sources differ most in their raw state and these differences were significantly reduced after processing. This indicates that both processing and array-based solutions can compensate well for the effect of the source ghost. Nevertheless, a small improvement in signal-to-noise ratio was found for

the broadband source dataset with respect to the standard source at frequencies around the standard source's ghost notch, which provided a modest uplift for high-resolution imaging of the shallow geology.

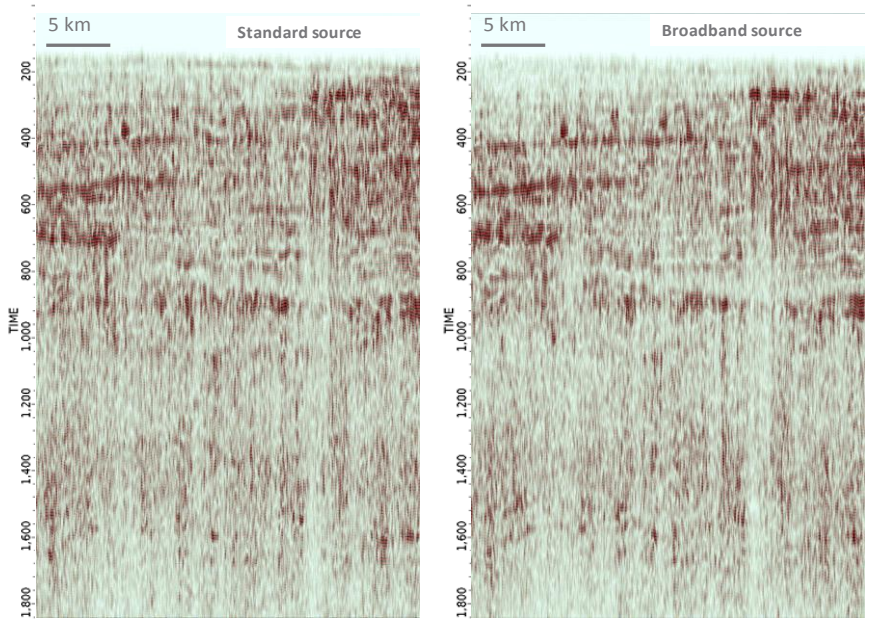

Figure 4 *– PSTM stack for standard source (left) and broadband source (right) showing the differences in imaging quality in a narrow-band, 107±5 Hz, corresponding to the location of the standard source ghost notch.*

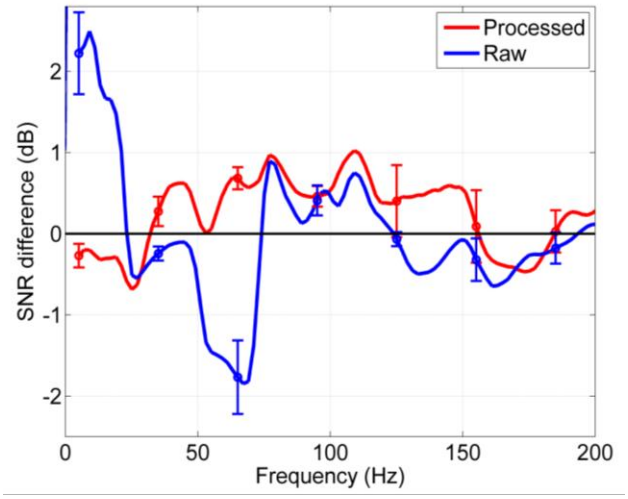

Figure 5 *–Signal-to-noise ratio differences estimated as a function of frequency before (blue curve) and after (red curve) processing for the two datasets. The estimation is carried out in 10 Hz bands using predictability calculated over ± 8 time lags and averaged over spatial cross-correlations of trace pairs between 6.25 and 300 m. Error bars are shown every 30 Hz.*

Acknowledgements

The data shown are provided courtesy of Dolphin's Multi-Client Department.

References

Kragh, E. and Christie, P. [2012] Seismic repeatability, normalized rms, and predictability, *The Leading Edge* 640-647

Parkes, G. and Hegna, S., [2011] A marine seismic acquisition system that provides a full 'ghost-free' solution, *81st Annual International Meeting*, SEG Expanded abstracts, 37-41

Siliqi, R., Payen T., Sablon, R. and Desrues, K. [2012] Synchronized multi-level source, a robust broadband marine solution, 82nd Annual International Meeting, *SEG Expanded abstracts*, 56-60